Equilibrium and growth morphology of oligoacenes: PBC analysis of naphthalene, anthracene and pentacene crystals

MASSARO F. R.; MORET M.; BRUNO M.; AQUILANO D.. Equilibrium and growth morphology of oligoacenes: PBC analysis of naphthalene, anthracene and pentacene crystals. CRYSTAL GROWTH & DESIGN. 12 pp: 982-989.
DOI: 10.1021/cg201458g

Equilibrium and growth morphology of oligoacenes: PBC analysis of naphthalene, anthracene and pentacene crystals

Francesco Roberto Massaro,[1] Massimo Moret,[1] Marco Bruno[2] and Dino Aquilano[2]*

[1] Dipartimento di Scienza dei Materiali - Università di Milano Bicocca, via R. Cozzi 53, I-20125 Milano, Italy.

[2] Dipartimento di Scienze Mineralogiche e Petrologiche - Università di Torino, via Valperga Caluso 35, I-10125 Torino, Italy.

* *corresponding author : roberto.massaro@mater.unimib.it*

Abstract:
The athermal equilibrium and growth crystal shapes of a series of oligoacenes, namely naphthalene, anthracene and pentacene, were simulated, in vacuum, by using three different sets of empirical potentials (UNI, UFF and MM3 force fields). By applying the Hartman-Perdok method of the periodic bond chains (PBC), the surface profiles were obtained, providing the specific surface and attachment energy values, both for ideal and relaxed surfaces. Very good agreement among the three force fields employed was observed. From calculations it ensues that surface relaxation only weakly affects surface and, even more, attachment energies of these semiconductor molecular crystals. It is noteworthy to point out that both equilibrium and growth shapes of these crystals are quite similar when concerning phases belonging to the same point group.

1. Introduction

Organic π-conjugated molecules are currently thoroughly investigated owing to their semiconducting properties as they could represent a valid substitute for inorganic semiconductors in the future.[1-4] Among organic semiconductors, oligoacenes, and in particular tetracene, pentacene, and their derivates, show the highest charge mobilities and thus represent promising materials for applications in organic electronic and optoelectronic devices.[5-9]

Physical characterization of these organic materials involves production of both single crystals and thin films, respectively to study the material intrinsic properties and to build fully operating devices. In this respect, crystal morphology is one of the most critical issues on determining easy processing

and exploitation of the material, An unsuitable crystal morphology can hamper the study or use of the selected molecule because of unavailability of crystal faces for studying anisotropy of physical properties in single crystals or due to performance degradation in thin films, e.g. decreased charge carrier mobilities due to grain boundaries.[10] Hence, in recent years many efforts were directed at improving growth techniques of organic semiconductors which quite often are difficult materials when trying to grow high quality single crystals or thin films.[11,12] A fundamental help to this purpose can be found in the analysis of the role exerted by the crystal structure on determining crystal morphology.

Recently, few papers treated the modeling of equilibrium crystal morphology and calculation of surface energies of organic semiconductors belonging to the oligoacenes, oligothiophenes and polyphenylenes classes.[13-17] One of these papers in particular[17] treated the calculation of surface energy and equilibrium crystal morphology of an extensive series of molecules covering several oligomers for the three cited chemical classes. However, as already noted in our previous paper on the subject,[18] there was no systematic approach for determining all possible forms involved in the equilibrium crystal morphologies but only an a priori choice of few low indexes crystal faces was considered. Moreover, the experimental growth shape cannot be directly compared to the calculated equilibrium shape since it is the morphology obtained through calculation of the attachment energies that must be compared to grown crystals.

At variance, the present work is part of a set of systematic studies dedicated to the prediction of the equilibrium, but also of the growth, crystal morphology of molecular compounds known for their semiconducting properties. The present approach is based on the detailed analysis and classification of the intermolecular interactions together with the character of the crystal faces according to the periodic bond chain (PBC) theory by Hartman and Perdock,[19-21] supplied by computer simulations through empirical atom-atom potentials. Our calculations about tetracene[18] proved that, for both the theoretical equilibrium and growth shapes, it is sufficient to take into account the molecular interactions belonging to the 1st order of magnitude (with all the related PBC ranks), being aware that minor faces could originate from calculations in the range of lower energies. Therefore, we extend this systematic approach to the study of other organic systems belonging to the oligoacenes class, completing the series from naphthalene to pentacene in order to evidence similarities and trends within a homologous series of compounds.

2. Computational Details

More details can be found in the previous paper.[18] Different computer codes coupled to three different sets of empirical potentials were used for performing the calculations and at the same time verifying the consistency of results, thus obtaining different energetic quantities not all available from experiments. The three computer codes adopted are described immediately below.

- The CSEHP (Crystal Site Energy according to Hartman and Perdok)[22,23] program is a home made code. We chose to include in our code the UNI[24,25] force field, principally to evaluate the intermolecular interactions, the end chain energy (*ECE*, the energy released when a molecule enters, in a crystallographic position, at one end of a semi-infinite PBC) of the PBCs, the specific surface energy (γ_{hkl}) and the attachment energy (E_{att}^{hkl}). Only unrelaxed surface energies were calculated, as CSEHP does not allow the optimization of the surface structure.

- Other calculations, mainly optimization of slab geometries and surface energy estimates, were carried out by using the UFF[26] molecular potentials implemented in the GULP 3.4 package (General Utility Lattice Program).[27] Bulk and slab geometry optimizations were performed by means of the Newton-Raphson method and considered converged when the gradient tolerance and the function tolerance (*gtol* and *ftol* adimensional parameters in GULP) were smaller than 0.0001 and 0.00001, respectively.

All surfaces were studied by using the 2D-slab model[28] where *hkl* slabs of varying thickness were obtained by separating the bulk structure along the plane of interest. Calculations were performed by considering the original 1×1 surface cell and the slab subdivided into two regions:

- region 1, containing both the surface and the underlying layers that are allowed to relax;
- region 2, having the same number of layers as region 1 and containing the rest of the slab material where no relaxation, with respect to the bulk crystal structure, is assumed to occur.

Calculations were done by considering slabs with thickness up to eight layers (four for each region), which are sufficient to reproduce bulk-like properties at the centre of the slab and to obtain a careful description of the surface.

The γ_{hkl} values were evaluated from the energy of the surface block (U_s, region 1) and the energy of a portion of bulk crystal (U_b, region 2) containing the same number of atoms as the surface block.[29] Both energies are referred to A_{hkl}, the common surface area of the primitive unit cell:

$$\gamma_{hkl} = (U_s - U_b) / A_{hkl}$$

E_{att}^{hkl} was calculated by adopting the following relation:

$$E_{att}^{hkl} = U_{tot}^{n+1} - U_{tot}^{n} - U_{tot}^{1}$$

where U_{tot}^{n} is the total internal energy of a surface model consisting of *n* growth layers, while U_{tot}^{1} is the energy of the growth layer alone.

- The last set of simulations were based on the MM3 force field[30,31] and carried out with the TINKER 4.2 molecular modeling package[32] which allows optimization of slab geometries and surface energy calculations. The Newton minimization was used with a rms gradient of 0.0001 kcal mol^{-1} $Å^{-1}$ and a 45 Å cutoff value for the van der Waals (vdW) interactions.

The lattice parameters were optimized by means of Xtalmin program included in the TINKER package. The surfaces were cut from the optimized bulk structure according to the *hkl* planes of interest; calculations were performed by adopting simple 1×1 2D surface cells. No super-cells were used in our calculations. The 3D slab model consisted of slabs of selected thickness stacked along a given direction and separated by vacuum gaps large enough for the vdW interactions between slabs to be negligible (i.e. beyond the cutoff value). For the calculation of the γ_{hkl} we adopted the relation:

$$\gamma_{hkl} = (E_s - E_b) / 2 A_{hkl}$$

where E_s is the optimized slab energy, E_b is the energy of an equivalent number of fixed bulk molecules and A_{hkl} is the area of the 2D surface cell. The thickness of the *hkl* slabs was progressively increased until the γ_{hkl} value reached convergence.

3. Methodology

This study adopts a multistage methodology we devised and validated in a previous work,[18] which is briefly described hereafter. The whole work has its roots in the PBC analysis, in the sense of Hartman and Perdok,[19-21] which consists of identifying the crystallographic directions [*uvw*] characterized by strong interactions among molecules. Such directions rule the character of the {*hkl*} forms, which can be F (flat), S (stepped) or K (kinked), depending on how many PBCs run in a slice of thickness d_{hkl} allowed by the extinction rules, thus influencing the morphology of a crystal.[19-21]

The first step includes the evaluation of the molecular interactions inside the crystal bulk. Once quantified, these energy values can be graded in different "bond orders" starting from the most attractive interaction. Starting from the results of our study of tetracene,[18] we chose to consider for the present work just the molecular interactions belonging to the 1st order of magnitude, namely those ranging from the strongest one down to the one representing 10% of the highest interaction energy.

The second step consists of verifying the existence of PBCs inside the bulk structure starting from the directions identified by the strongest intermolecular bonds and proceeding with those built by more than one strong interaction (in this case the direction of the PBC does not coincide with that of the bonds). Once all the likely PBCs are detected, *ECE*s are calculated and a hierarchy based on the *ECE* order of magnitude is established ("PBC rank" hereafter). All {*hkl*} forms that originated from the identified PBCs are then classified as F, S or K. Therefore, starting from the 1st PBC rank, F_1, S_1 and K_1 forms appeare, followed by periodic chains of lower ranks.

In the following step, the specific surface energies were calculated by means of the chosen potentials. The couples GULP-UFF and TINKER-MM3 allowed us to introduce surface relaxation to produce more realistic morphologies. The couples CSEHP-UNI and GULP-UFF, allowed us to

calculate the E_{att}^{hkl} as well, by which approximate linear growth rates (R^{hkl}) of the crystal forms could be estimated, according to the relation: $R^{hkl} \propto E_{att}^{hkl}$.[33]

4. Results and discussion

4.1 The equilibrium shape (ES)

Starting from the crystal structures of naphthalene (space group $P2_1/a$; a_0 = 8.010 b_0 = 5.884, c_0 = 8.536 Å; α = 90, β = 123.45, γ = 90°; Z = 2),[34] anthracene (space group $P2_1/a$; a_0 = 8.5526 b_0 = 6.0158, c_0 = 11.1720 Å; α = 90, β = 124.596, γ = 90°; Z = 2)[35] and pentacene (space group $P\bar{1}$; a_0 = 6.265 b_0 = 7.786, c_0 = 14.511 Å; α = 76.65, β = 87.50, γ = 84.61°; Z = 2),[36] we could estimate the surface energies for all {*hkl*} forms originated from their pertinent PBCs. Utilizing them in the Gibbs-Wulff's construction,[37] the corresponding crystal ES were obtained.

4.1.1 Naphthalene

When considering the 1st order intermolecular bonds,[18] it is possible to number 5 vdW interactions (Table 1) and 8 PBCs (Table 2) in the naphthalene crystal structure, 5 matching strong molecular directions and 3 arising from a composition of more bonds. In Table 2 the *ECE* of these PBCs calculated with CSEHP are reported, each of them belonging to the 1st PBC rank.[18]

Table 1. The molecular interactions issued from the first bond order in naphthalene. The calculations were performed by means of program-potential CSEHP-UNI.

molecule label	molecule label	distance [Å]	direction	interaction [kJ/mol]	bond label
1	2	4.969	**[1 1 0]**	-17.6	a
1	1	5.884	**[0 1 0]**	-12.3	b
1	2	7.738	**[1 1 2]**	-4.9	c
1	1	8.536	**[0 0 1]**	-4.0	d
1	1	7.852	**[1 0 1]**	-2.2	e

Table 2. PBC end chain energies (*ECEs*) relative to the 1st bond order intermolecular interactions in naphthalene. Directions corresponding to 1st order molecular bonds are quoted with an asterisk. The "bonds" column shows the name of the intermolecular bonds forming the PBCs.

PBC	PBC rank	bonds	*ECE* [erg / molecule]
[0 1 0]*	1	a + a'	-3.64×10^{-13}
[0 0 1]*	1	a + c	-2.16×10^{-13}
[1 0 0]	1	a + a'	-1.86×10^{-13}
[0 1 1]	1	a + c' (a'+c)	-1.69×10^{-13}
[1 1 0]*	1	a (a')	-1.61×10^{-13}
[1 0 1]*	1	a + c' (a'+c)	-1.54×10^{-13}
[1 1 1]	1	a + c' (a'+c)	-5.03×10^{-14}

[1 1 2]*	1	c (c')	-4.13 x 10^{-14}

Fourteen crystallographic forms are generated by the aforementioned PBCs, of which six are F_1 forms, while eight are S_1. Table 3 shows these 14 forms classified and ordered according to their PBC rank and specific surface energy. As already ascertained in the previous paper about tetracene,[18] fairly good agreement is evident by comparing values obtained with different force fields. The energy difference percentage: $\Delta_{UR} = (\gamma^{relaxed}-\gamma^{unrelaxed})/\gamma^{unrelaxed}$, between relaxed and unrelaxed surfaces is also indicated in the UFF and MM3 columns for all forms. It is worth outlining the weak relaxation suffered in general by the surfaces: indeed, Δ_{UR} goes from minima of 0.4% with UFF and 0.6% with MM3 for the {001} form, to a maximum difference close to 9% in just one case. The average Δ_{UR} are in good agreement, being 1.6% and 2.6% for UFF and MM3, respectively.

Table 3. Naphthalene specific surface energies for the 14 crystallographic forms arising from 1st bond order interactions. Forms with MRI ≥ 1.0% are quoted with an asterisk. Values are expressed in erg/cm^2 and ordered by relaxed γ values calculated with UFF.

		UNI	UFF			MM3		
character	**form**	$\gamma_{unrelaxed}$	$\gamma_{unrelaxed}$	$\gamma_{relaxed}$	Δ_{UR}	$\gamma_{unrelaxed}$	$\gamma_{relaxed}$	Δ_{UR}
F_1	**{0 0 1}***	81.9	96.5	96.1	-0.4%	81.5	81.0	-0.6%
F_1	**{1 1 0}***	110.2	112.5	111.0	-1.3%	115.7	105.4	-8.9%
S_1	**{2 0 0}***	109.0	114.2	112.2	-1.8%	103.1	100.6	-2.4%
F_1	**{2 0 $\bar{1}$}***	112.4	114.9	112.7	-1.9%	101.8	99.2	-2.6%
S_1	**{3 1 $\bar{1}$}***	120.3	123.6	121.7	-1.5%	111.6	109.8	-1.6%
S_1	**{1 1 1}***	112.4	122.4	122.1	-0.2%	113.3	108.8	-4.0%
F_1	**{1 1 $\bar{1}$}***	118.1	126.3	124.5	-1.4%	109.6	107.3	-2.1%
F_1	**{2 1 $\bar{1}$}**	125.5	131.3	128.3	-2.3%	116.6	114.1	-2.1%
S_1	**{3 1 $\bar{2}$}***	126.7	133.5	131.2	-1.7%	116.1	113.6	-2.2%
S_1	**{2 0 $\bar{2}$}***	126.8	142.3	138.1	-3.0%	116.0	113.9	-1.8%
S_1	**{1 1 $\bar{2}$}***	123.2	141.1	138.8	-1.6%	117.1	114.4	-2.3%
S_1	**{0 2 0}***	131.7	141.8	139.3	-1.8%	122.0	119.8	-1.8%
S_1	**{0 2 1}**	130.9	142.4	139.9	-1.8%	122.1	119.4	-2.2%
F_1	**{0 1 1}**	130.4	146.0	142.9	-2.1%	124.6	122.2	-1.9%

For quantitatively describing crystal morphologies, we evaluated the morphological relevance index (MRI) for all the {*hkl*} forms, defined as the percent ratio between the total area of the faces belonging to a {*hkl*} form and the total surface area of the crystal. The MRI gives an immediate and quantitative estimation of the abundance of the crystallographic forms belonging to the crystal habit, and then a starting point to study the interactions between the crystal and its surroundings. The {*hkl*} forms in Table 3 marked with an asterisk are forms having MRI ≥ 1.0% which enter the final equilibrium morphology. By color coding the crystal faces according to their character (green for F, yellow for S and red for K faces) an effective and useful representation of the crystal morphology can be easily provided. Figure 1 clearly outlines that the main forms ({001}, {110},

{11$\bar{1}$}, {20$\bar{1}$}) all exhibit an F character but at the same time S forms are not negligible. Apart from a few narrow faces placed between F faces, in fact, some S forms are noteworthy with a MRI > 6% as it is the case for {200}. Simulations performed with different force fields lead to morphologies that are very similar for both the index and the relative surface area of the faces. Only minor differences appear such, e.g., the S character of the faces more evident with the MM3 force field.

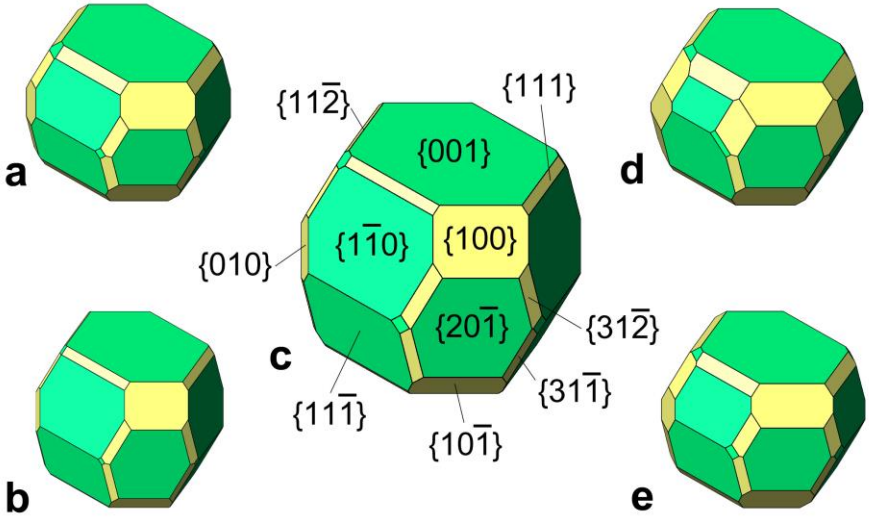

Figure 1 – Naphthalene equilibrium morphology from the 1st order molecular interactions. The crystal morphologies are from calculations performed by means of UNI (a), UFF without (b) and with surface relaxation (c) and MM3 without (d) and with surface relaxation (e). Drawing (c) reports indexes only for those crystallographic forms having MRI ≥ 1.0%.

4.1.2 Anthracene

It is possible to identify 4 vdW strong interactions (Table 4) and 8 PBCs in the anthracene crystal structure, 4 matching strong molecular directions and 4 arising from a composition of more bonds. Table 5 shows that each PBC belongs to the 1st PBC rank.

Table 4. The molecular interactions issued from the first bond order in anthracene. The calculations were performed by means of program-potential CSEHP-UNI.

molecule label	molecule label	distance [Å]	direction	interaction [kJ/mol]	bond label
1	2	5.228	**[1 1 0]**	-27.1	a
1	1	6.016	**[0 1 0]**	-17.9	b
1	2	9.894	**[1 1 2]**	-6.8	c
1	1	11.172	**[0 0 1]**	-4.5	d

Table 5. PBC end chain energies (*ECEs*) relative to the 1st bond order intermolecular interactions in anthracene. Directions corresponding to 1st order molecular bonds are quoted with an asterisk.

PBC	PBC rank	bonds	*ECE* [erg / molecule]
[0 1 0]*	1	a + a'	-5.41 x 10^{-13}

[0 0 1]*	1	a + c	-3.02 x 10^{-13}
[1 0 0]	1	a + a'	-2.56 x 10^{-13}
[0 1 1]	1	a + c' (a'+c)	-2.38 x 10^{-13}
[1 1 0]*	1	a (a')	-2.36 x 10^{-13}
[1 0 1]	1	a + c' (a'+c)	-9.41 x 10^{-14}
[1 1 1]	1	a + c' (a'+c)	-6.61 x 10^{-14}
[1 1 2]*	1	c (c')	-5.65 x 10^{-14}

Exactly as in naphthalene, 14 crystallographic forms are generated from the set of 8 PBCs; in detail, 6 are F_1 and 8 are S_1 forms (see Table 6). UNI and MM3 potentials give surface energies in close agreement, while the UFF originates slightly higher γ values. Δ_{UR} goes from minima of 0.3% with UFF and 2.5% with MM3 for the {001} form, to a maximum difference of 3.3% for $\{11\bar{2}\}$. The average Δ_{UR} are 2.8% and 2.6% for UFF and MM3, respectively.

Table 6. Anthracene specific surface energies for the 14 crystallographic forms arising from 1st bond order interactions. Forms with MRI ≥ 1.0% are quoted with an asterisk. Values are expressed in erg/cm^2 and ordered by relaxed γ values calculated with UFF. The boxes with no results indicate calculations that did not reach convergence.

		UNI	UFF			MM3		
character	**Form**	$\gamma_{unrelaxed}$	$\gamma_{unrelaxed}$	$\gamma_{relaxed}$	Δ_{UR}	$\gamma_{unrelaxed}$	$\gamma_{relaxed}$	Δ_{UR}
F_1	**{0 0 1}***	85.9	96.9	96.6	-0.3%	83.6	81.5	-2.5%
F_1	**{1 1 0}***	111.3	118.6	115.1	-3.0%	111.6	108.4	-2.9%
S_1	**{2 0 0}***	112.8	119.7	117.0	-2.3%	110.6	107.8	-2.5%
F_1	**{1 1 $\bar{1}$}***	122.1	122.4	119.5	-2.4%	119.0	115.7	-2.8%
S_1	**{1 1 1}***	116.8	127.0	123.6	-2.7%	116.7	114.0	-2.3%
S_1	**{3 1 $\bar{1}$}***	123.1	130.3	127.1	-2.5%	-	-	-
F_1	**{2 0 $\bar{1}$}***	115.5	133.7	129.8	-2.9%	111.0	108.4	-2.3%
F_1	**{2 1 $\bar{1}$}**	128.5	137.6	132.8	-3.5%	125.8	122.6	-2.5%
S_1	**{3 1 $\bar{2}$}***	131.8	141.6	137.9	-2.6%	-	-	-
S_1	**{0 2 0}**	134.4	150.6	145.2	-3.6%	132.4	129.2	-2.4%
S_1	**{2 0 $\bar{2}$}***	139.5	154.3	146.6	-5.0%	-	-	-
S_1	**{0 2 1}**	134.7	152.1	148.2	-2.6%	132.8	129.5	-2.5%
S_1	**{1 1 $\bar{2}$}**	135.1	154.9	150.1	-3.1%	130.6	126.3	-3.3%
F_1	**{0 1 1}**	138.4	157.3	152.4	-3.1%	136.1	132.6	-2.6%

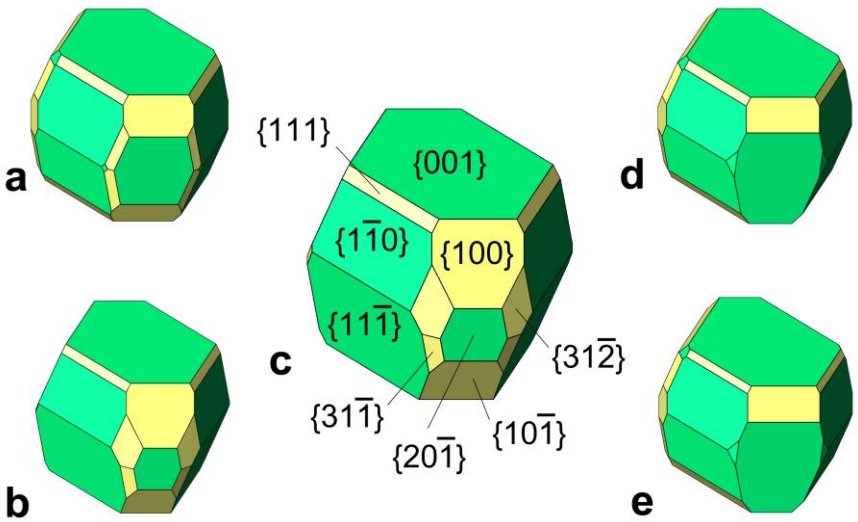

Figure 2 – Anthracene equilibrium morphology from the 1st order molecular interactions. The crystal morphologies are from calculations performed by means of UNI (a), UFF without (b) and with surface relaxation (c) and MM3 without (d) and with surface relaxation (e). Drawing (c) reports indexes only for those crystallographic forms having MRI ≥ 1.0%.

Figure 2 reveals that in the case of anthracene the three main forms ({001}, {110}, {11$\bar{1}$}), together representing almost 70% of the crystal surface, all exhibit an F character, while the total MRI of the S forms is about 20%. The most important S form is again the {200} with a MRI = 7.5%. Apart from differences caused by the lack of MM3 data about some minor faces, morphologies simulated with the three force fields lead to shapes that are definitely comparable.

4.1.3 Pentacene

Pentacene crystal structure exhibits 4 vdW strong interactions (Table 7) and 11 PBCs in the 1st order of molecular forces. The *ECE* of these periodic boundary chains are quoted in Table 8: eight of them belong to the 1st PBC rank, one to the 2nd and two to the 3rd one.

Table 7. The molecular interactions issued from the first bond order in pentacene. The calculations were performed by means of program-potential CSEHP-UNI.

molecule label	molecule label	distance [Å]	direction	interaction [kJ/mol]	bond label
1	2	4.762	**[1 $\bar{1}$ 0]**	-51.9	a
1	2	5.221	**[1 1 0]**	-48.4	b
2	2	6.265	**[1 0 0]**	-30.3	c
2	2	14.414	**[1 1 $\bar{2}$]**	-7.0	d

Table 8. PBC end chain energies (*ECEs*) relative to the 1st bond order intermolecular interactions in pentacene. Directions corresponding to 1st order molecular bonds are quoted with an asterisk.

PBC	PBC rank	bonds	*ECE* [erg / molecule]
[1 0 0]*	1	a + b	-1.36 x 10^{-12}
[0 1 0]	1	a + b	-4.80 x 10^{-13}
[1 1 $\bar{1}$]	1	b + d	-4.60 x 10^{-13}
[1 $\bar{1}$ 0]*	1	a	-4.59 x 10^{-13}
[0 0 1]	1	b + d	-4.44 x 10^{-13}
[1 1 0]*	1	b	-4.26 x 10^{-13}
[1 0 $\bar{1}$]	1	a + d	-4.21 x 10^{-13}
[0 1 $\bar{1}$]	1	a + d	-1.46 x 10^{-13}
[1 1 $\bar{2}$]*	2	d	-5.82 x 10^{-14}
[1 $\bar{1}$ 2]	3	c + d	-7.61 x 10^{-15}
[3 1 $\bar{2}$]	3	c + d	-1.92 x 10^{-15}

Nineteen crystallographic forms are thus generated by the aforementioned PBCs (see Table 9); more specifically there are 8 forms with flat character (seven F_1 and one F_2), 5 forms with stepped

character (four S_1 and one S_2) and 6 kinked forms (all K_3). UNI and UFF energies well agree, while the surface energy values calculated with MM3 force field are constantly lower. Δ_{UR} goes from minima of 1.8% with UFF and 2.0% with MM3, to a maximum of 4.7%; the average Δ_{UR} value is 2.7% for both UFF and MM3. Hence, summarizing data obtained for naphthalene, anthracene, tetracene, and pentacene no dramatic surface relaxation does in general occur, especially for closed packed surfaces comprising the monomolecular layer comprising the herring-bone motif.

Table 9. Pentacene specific surface energies for the 19 crystallographic forms arising from 1st bond order interactions. Forms with MRI ≥ 1.0% are quoted with an asterisk. Values are expressed in erg/cm^2 and ordered by relaxed γ values calculated with UFF. The boxes with no results indicate calculations that did not reach convergence.

		UNI	UFF			MM3		
character	Form	$\gamma_{unrelaxed}$	$\gamma_{unrelaxed}$	$\gamma_{relaxed}$	Δ_{UR}	$\gamma_{unrelaxed}$	$\gamma_{relaxed}$	Δ_{UR}
F_1	**{0 0 1}***	80.9	82.7	81.2	-1.8%	72.1	70.0	-2.9%
F_1	**{0 1 1}***	128.9	128.1	125.6	-2.0%	122.3	119.9	-2.0%
S_1	**{1 1 2}***	127.1	129.1	125.6	-2.7%	122.6	119.0	-2.9%
F_1	**{1 $\bar{1}$ 0}***	127.9	129.6	126.7	-2.2%	122.0	118.5	-2.9%
F_1	**{1 1 1}***	130.1	132.5	128.9	-2.7%	124.4	120.3	-3.3%
F_2	**{0 2 1}***	134.6	134.0	131.1	-2.2%	125.3	122.6	-2.2%
S_1	**{$\bar{1}$ 1 1}***	132.1	134.8	131.1	-2.7%	125.7	122.1	-2.9%
K_3	**{$\bar{1}$ 3 2}**	139.3	139.7	136.9	-2.0%	132.8	129.7	-2.3%
K_3	**{1 3 3}**	141.7	140.6	137.7	-2.1%	133.5	130.1	-2.5%
S_1	**{1 $\bar{1}$ 1}***	136.0	142.6	138.1	-3.2%	128.8	125.5	-2.6%
F_1	**{0 1 0}***	148.1	150.5	143.4	-4.7%	136.2	132.8	-2.5%
K_3	**{1 $\bar{3}$ 0}**	181.2	151.1	147.3	-2.5%	139.0	135.7	-2.4%
S_1	**{1 1 0}***	151.7	155.9	150.7	-3.3%	140.9	135.9	-3.5%
K_3	**{1 3 1}**	156.1	157.7	152.6	-3.2%	145.0	140.6	-3.0%
F_1	**{1 0 1}**	151.4	161.5	156.2	-3.3%	145.2	141.2	-2.8%
S_2	**{2 0 1}**	152.4	162.3	158.1	-2.6%	145.4	141.7	-2.5%
K_3	**{2 0 3}**	150.5	163.0	159.0	-2.5%	-	-	-
F_1	**{1 0 0}**	160.2	170.5	165.7	-2.8%	151.7	147.9	-2.5%
K_3	**{2 0 $\bar{1}$}**	169.9	179.0	174.6	-2.5%	157.5	153.5	-2.5%

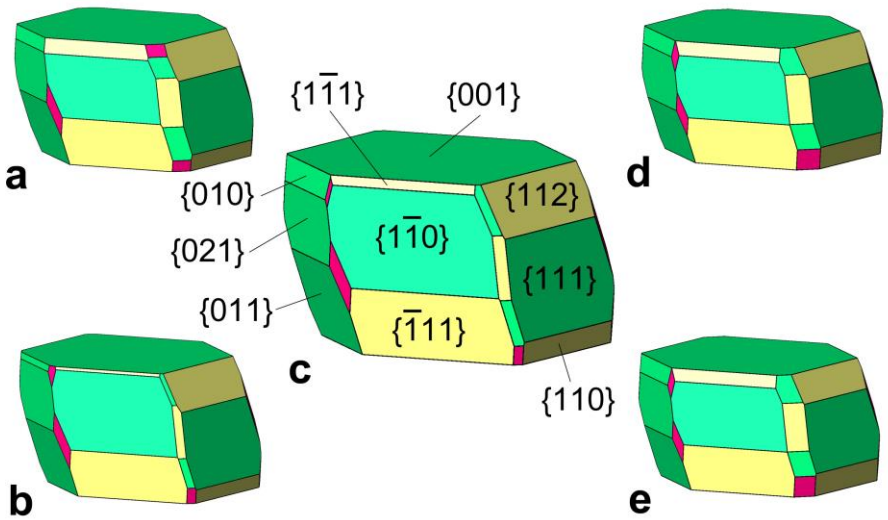

Figure 3 – Pentacene equilibrium morphology from the 1st order molecular interactions. The crystal morphologies are from calculations performed by means of UNI (a), UFF without (b) and with

surface relaxation (c) and MM3 without (d) and with surface relaxation (e). Drawing (c) reports indexes only for those crystallographic forms having MRI ≥ 1.0%.

Figure 3 shows that the {001} pinacoid, having MRI = 40%, is more relevant than in the previous cases. The total MRI of the stepped forms is just below 20%, the most important S forms being $\{\bar{1}11\}$ and {112}, with MRIs equal to about 8 and 7%, respectively. Unlike what happens with the other oligoacenes, it is noteworthy to mention the appearance of small K faces that reach 2% of the total crystal surface. Again, the accordance among the equilibrium shapes deriving from different calculations is good, in particular between UNI and UFF simulations.

Table 10. In the upper part the MRIs ≥ 1.0% of naphthalene, anthracene, tetracene[18] and pentacene resulting from the 1st bond order calculation are showed. In the lower part the total MRI referred to PBC categories and to the character of the faces. All data were calculated with UFF.

MRI	26.7% {001} 26.5% {110} 18.4% $\{11\bar{1}\}$ 10.6% $\{20\bar{1}\}$ 6.2% {200} 3.3% {111} 2.1% $\{20\bar{2}\}$ 2.0% $\{31\bar{1}\}$ 1.5% $\{31\bar{2}\}$ 1.0% {020}	26.8% {110} 26.3% {001} 17.9% $\{11\bar{1}\}$ 10.5% $\{20\bar{1}\}$ 6.4% {200} 2.7% $\{20\bar{2}\}$ 2.5% {111} 1.8% $\{31\bar{1}\}$ 1.4% $\{31\bar{2}\}$ 1.0% {020} 1.0% $\{11\bar{2}\}$	29.4% {001} 28.0% $\{11\bar{1}\}$ 19.7% {110} 7.5% {200} 3.8% $\{31\bar{1}\}$ 3.6% $\{20\bar{1}\}$ 3.3% $\{20\bar{2}\}$ 3.2% {111} 1.5% $\{31\bar{2}\}$	28.4% {001} 27.5% $\{11\bar{1}\}$ 20.3% {110} 7.5% {200} 4.3% $\{20\bar{2}\}$ 3.7% $\{31\bar{1}\}$ 3.7% {111} 3.5% $\{20\bar{1}\}$ 1.2% $\{31\bar{2}\}$	37.9% {001} 11.8% {112} 11.7% $\{1\bar{1}0\}$ 8.2% {111} 7.5% {021} 6.8% $\{1\bar{1}1\}$ 5.6% {011} 2.7% {010} 1.9% $\{\bar{1}11\}$ 1.6% {110}	37.3% {001} 11.9% $\{1\bar{1}0\}$ 11.6% {112} 8.1% {111} 7.3% {021} 6.6% $\{1\bar{1}1\}$ 5.6% {011} 2.8% {010} 2.2% $\{\bar{1}11\}$ 2.1% {110} 1.0% {101}	40.3% {001} 12.3% $\{1\bar{1}0\}$ 12.2% {111} 7.7% {011} 7.5% $\{\bar{1}11\}$ 6.8% {021} 6.6% {112} 2.0% {110}	39.7% {001} 11.9% {111} 11.5% $\{1\bar{1}0\}$ 7.9% $\{\bar{1}11\}$ 7.6% {011} 6.7% {112} 5.6% {021} 2.5% {110} 2.1% {010} 1.1% $\{1\bar{1}1\}$
phase	**naphthalene**		**anthracene**		**tetracene**		**pentacene**	
relaxation	no	yes	no	yes	no	yes	no	yes
PBC 1	100.0%	100.0%	100.0%	100.0%	71.8%	72.4%	90.3%	91.8%
PBC 2	–	–	–	–	28.2%	27.6%	7.4%	6.2%
PBC 3	–	–	–	–	–	–	2.3%	2.0%
F	82.5%	82.3%	80.7%	79.6%	92.8%	92.7%	80.6%	79.3%
S	17.5%	17.7%	19.3%	20.4%	7.2%	7.3%	17.2%	18.7%
K	–	–	–	–	–	–	2.3%	2.0%

Table 10 summarizes all the equilibrium morphology data about oligoacenes obtained in the present work and in reference [18]. It reports the MRI of all forms with surface extension ≥ 1.0% for every phase explored from naphthalene to pentacene; the weight of the character and the pertinent PBC rank is considered as well. This table supports some important conclusions:

- the {001} is absolutely the dominant form in tetracene and pentacene with a MRI near 40%; having MRI less than 30%, it co-dominates with the form {110} and $\{11\bar{1}\}$ in crystals of naphthalene and antracene, respectively;
- the forms arising from the 1st PBC rank and those with F character control the final ES, their MRI never going below about 70% and 80%, respectively;
- the entire surface of naphthalene and anthracene crystals is made of forms belonging to the 1st PBC rank;
- the heavier oligomers tetracene and pentacene start to show faces belonging to alternative PBC ranks: the 2nd for tetracene and the 2nd besides the 3rd for pentacene;
- in naphthalene, anthracene and pentacene F and S forms have more or less the same weight (about 80% and 20%, respectively);
- the F character weighs more (> 90%) in tetracene, while the S character is less important (< 10%);
- pentacene is the only species to have a little percentage of K forms (about 2%).

4.2 The growth shape (GS)

When trying to analyze and improve the results of growth experiments (both single crystals and thin films) there is the unavoidable need of simulating the growth morphology. We calculated with the same modeling tools the E_{att}^{hkl} relative to the crystallographic forms presented in the previous paragraphs. Figure 4 gives the E_{att} morphologies[33] of naphthalene, anthracene and pentacene, respectively, using the information in Tables S1-S3 in the Supporting Information.

A first striking feature is the growth habit fairly different from the equilibrium one: it is more tabular, particularly in pentacene, and dominated by the {001} form. Besides, the number of crystallographic forms in the growth shape is remarkably smaller with respect to the equilibrium shape, since no minor rounding faces do occur. Only five F forms enter the final growth morphology of naphthalene: {001}, {110}, $\{11\bar{1}\}$, $\{20\bar{1}\}$ and {011}; their MRIs, including surface relaxation, are 43.6, 24.3, 19.7, 11.5 and 0.9%, respectively. The growth morphology for anthracene contains the same five forms, with MRIs which become 52.4, 15.1, 20.4, 9.8 and 2.3%. Finally, in pentacene the F forms increase to seven: {001}, {011}, {100}, {111}, $\{1\bar{1}0\}$, {010} and {101}; the MRIs are 66.2, 13.0, 7.6, 5.7, 3.3, 3.1 and 1.1%, respectively. Here the {001} pinacoid weighs more than in the other smaller oligoacenes as can be deduced from the flattening of the crystal shape; this is an expected result from a detailed PBC analysis since the d_{001} layer includes four of the strongest PBCs in the structure, namely directions [100], [010], $[1\bar{1}0]$ and [110].

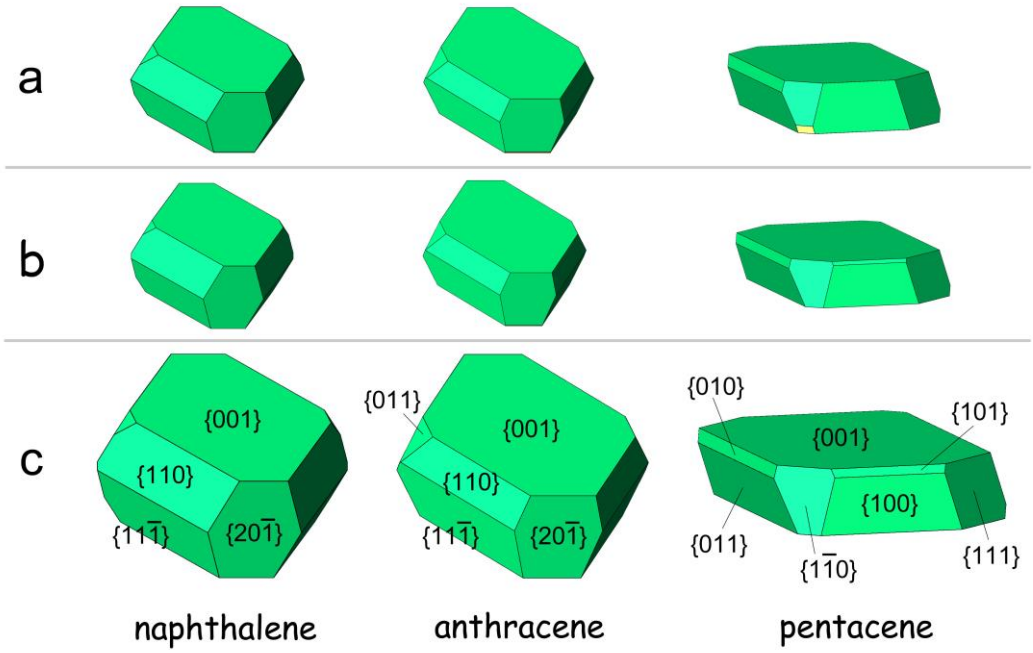

Figure 4 – Oligoacenes growth shapes from calculations performed by means of UNI (stripe a) and UFF without (stripe b) and with surface relaxation (stripe c) potentials. Stripe c reports indexes only for those crystallographic forms having MRI ≥ 1.0%.

E_{att}^{hkl} changes due to surface relaxation, that we estimated by the quantity $\Delta_{EAR} = (E_{att}^{relaxed} - E_{att}^{unrelaxed})/E_{att}^{unrelaxed}$, are always lower than the γ changes. In naphthalene the Δ_{EAR} mean value is 0.7% with small discrepancies among F (0.4%) and S (0.9%) forms. For anthracene the mean value is 0.9% with differences among F (0.4%) and S (1.3%) forms. In pentacene the mean value is 0.9% with differences among F (0.5%), S (0.7%) and K (1.8%) forms.

The crystallographic form which is less modified by introducing surface relaxation is again {001} showing Δ_{EAR} = 0.0% in all the three crystals. This happens since the d_{001} slice contains the highly compact herring-bone packing motif typical of the family of oligoacenes. As a consequence, all experimentalists confront themselves with the difficulty of growing oligoacenes {001}-thick crystals.

The results concerning naphthalene, anthracene and tetracene[18] definitely agree with the E_{att} morphologies simulated by Cuppen and coworkers,[15] who performed simulations utilizing the Dreiding force field in combination with ESP derived point charges.

For what concerns the comparison to experimental morphology, our results definitely agree with previous works. In paper [13,16] experimental growth morphologies are reported: naphthalene, anthracene and pentacene crystals, grown from vacuum sublimation, show habits dominated by the {001}, as in our simulations. In detail, the agreement with the computational and experimental study about naphthalene and anthracene[13] is almost perfect.

5. Conclusions

We used computationally cheap simulation methods to perform a morphological study about three member of the oligoacenes class, definitely confirming the results achieved in a recent methodological paper about tetracene.[18] Results obtained by using different force fields led to nearly identical equilibrium and growth shapes, in addition to a few general conclusions. The shapes from our simulations are richer in crystallographic forms (especially the equilibrium shape) compared to those recently appeared in the literature.[14,16,17] More than the use of computationally expensive calculations, we believe it is necessary to perform a preparatory deep PBC analysis, to avoid the arbitrary assumption that only low index surfaces enter the final morphology of crystals. Moreover, we observed that surface relaxation weakly affects surface and, even less, attachment energies of molecular crystals; this behavior somewhat differs from what we observed with ionic structures.[38-41] This result is of relevance for the promising computer simulations of organic-organic crystalline interfaces with evaluation of epitaxial relations and adhesion energies,[42-45] setting a sound basis about the assumption of negligible relaxation for low energy surfaces.

As seen with tetracene,[18] crystalline oligoacenes have many forms with similar specific surface energies. This implies that the equilibrium morphologies are densely facetted and strongly influenced by the point group. As a demonstration, the predicted ES (but also the GS) of naphthalene and antracene, which belong to the monoclinic prismatic class 2/m, are very similar. The same happens with tetracene and pentacene, which are members of the triclinic pinacoidal class $\bar{1}$; in this case the habit is less equidimensional, but rather barrel-like: one form, the {001}, rules over the other ones and several faces roughly belong to the zone axis perpendicular to the dominant form. The calculated crystal shapes, in primis the growth shape, reveal that oligoacenes crystals are strongly influenced by the structural arrangement of their herring-bone packing motif. Invariably, all the predicted GS turn out to be flattened according to the {001} form, the d_{001} containing the highly compact herring-bone packing. In terms of Hartman-Perdok theory, this means that the d_{001} includes the strongest PBCs of the structure, and this is even more true for tetracene and pentacene which own the longest polycyclic core.

Supporting Information Available. Tables listing the attachment energies of naphthalene (S1), anthracene (S2) and pentacene (S3).

References

(1) Braga, D.; Horowitz G. *Adv. Mater.* **2009**, *21*, 1473–1486.

(2) Witte, G.; Wöll, C. *J. Mater. Res.* **2004**, *19*, 1889-1916.

(3) de Boer, R. W. I.; Gershenson, M. E.; Morpurgo, A. F.; Podzorov, V. *Phys. Stat. Sol.* **2004**, *201*, 1302-1331.

(4) Reese, C.; Bao, Z. *J. Mater. Chem.* **2006**, *16*, 329-333.

(5) Anthony, J. E. *Angew.Chemie Int. Ed.* **2007**, *46*, 452-483.

(6) de Boer, R. W.; Klapwijk, T. M.; Morpurgo, A. F. *Appl. Phys. Lett.* **2003**, *83*, 4345.

(7) Verlaak, S.; Cheyns, D.; Debucquoy, M.; Arkhipov, V.; Heremans, P. *Appl. Phys. Lett.* **2004**, *85*, 2405.

(8) Pivovar, A. M.; Curtis, J. E.; Leao, J. B.; Chesterfield, R. J.; Frisbie, C. D. *Chemical Physics* **2006**, *325*, 138.

(9) Podzorov, V.; Menard, E.; Borissov, A.; Kiryukhin, V.; Rogers, J. A.; Gershenson, M. E. *Phys. Rev. Lett.* **2004**, *93*, 086602.

(10) Lunt, R. R.; Benziger, J. B.; Forrest, S. R. *Adv. Mater.* **2010**, *22*, 3857–3875.

(11) Laudise, R. A; Kloc, Ch.; Simpkins, P. G.; Siegrist T. *J. Crystal Growth* **1998**, *187*, 449-454.

(12) Campione, M.; Moret, M.; Raimondo, L.; Sassella A. *J. Phys. Chem. C* **2009**, *113*, 20927-20933.

(13) Grimbergen, R. F. P.; Reedijk, M. F.; Meekes, H.; Bennema P. *J. Phys. Chem. B* **1998,** *102*, 2646-2653.

(14) Northrup, J. E.; Tiago, M. L.; Louie S. G. *Phys. Rev. B* **2002**, *66*, 121404.

(15) Cuppen, H. M.; Graswinckel, W. S.; Meekes, H. *Cryst. Growth Des.* **2004**, *4*, 1351-1357.

(16) Drummy, L. F.; Miska, P. K.; Alberts, D.; Lee, N.; Martin D. C. *J. Phys. Chem. B* **2006,** *110*, 6066-6071.

(17) Nabok, D.; Puschnig, P.; Ambrosch-Draxl C. *Phys. Rev. B* **2008**, *77*, 245316.

(18) Massaro, F. R.; Moret, M.; Bruno, M.; Rubbo, M.; Aquilano, D. *Cryst. Growth Des.* **2011**, *11*, 4639-4646.

(19) Hartman, P.; Perdok W.G. *Acta Crystallogr.* **1955**, *8*, 49-52.

(20) Hartman, P.; Perdok W.G. *Acta Crystallogr.* **1955**, *8*, 521-525.

(21) Hartman, P.; Perdok W.G. *Acta Crystallogr.* **1955**, *8*, 525-529.

(22) Aquilano, D.; Rubbo, M.; Catti, M.; Pavese, A. *J. Cryst. Growth* **1997**, *182*, 168-184.

(23) Rubbo, M.; Aquilano, D. *J. Cryst. Growth* **1998**, *194*, 156-159.

(24) Filippini, G.; Gavezzotti, A. *Acta Crystallogr. B* **1993**, *49*, 868-880.

(25) Gavezzotti, A. *Molecular aggregation: structure analysis and molecular simulation of crystals and liquids.* Oxford University Press: New York, 2007.

(26) Rappé, A. K.; Casewit, C. J.; Colwell, K. S.; Goddard III, W. A.; Skiff, W. M. *J. Am. Chem. Soc.* **1992**, *114*, 10024-10035.

(27) Gale, J. D. *J. Chem. Soc. Faraday Trans.* **1997**, *93*, 629-637.

(28) Dovesi, R.; Civalleri, B.; Orlando, R.; Roetti, C.; Saunders, V. R. In *Reviews in Computational Chemistry*; Lipkowitz, B.K.; Larter, R.; Cundari, T. R., Eds.; John Wiley and Sons Inc.: New York, 2005; Vol. 21, pp 1-125.

(29) Gale, J. D. General Utility Lattice Program User's Manual, Curtin University of Technology, Perth, Australia.

(30) Allinger, N. L.; Yuh, Y. H.; Lii, J.-H. *J. Am. Chem. Soc.* **1989**, *111*, 8551-8566.

(31) Lii, J.-H.; Allinger, N. L. *J. Am. Chem. Soc.* **1989**, *111*, 8566-8575.

(32) Ponder, J. W. Tinker. Software tools for molecular design. Version 4.2, June 2004.

(33) Hartman, P.; Bennema, P. *J. Cryst. Growth* **1980**, *49*, 145-156.

(34) Alt, H.C.; Kalus, J. *Acta Crystallogr. B* **1982**, *38*, 2595.

(35) Brock, C.P.; Dunitz, J.D. *Acta Crystallogr. B* **1990**, *46*, 795.

(36) Siegrist, T,; Kloc, C.; Schon, J.H.; Batlogg, B.; Haddon, R.C.; Berg, S.; Thomas G.A. *Angew. Chem.* **2001**, *40*, 1732.

(37) Kern, R. In *Morphology of crystals Part A*; Sunagawa, I., Ed.; Terra Scientific Publishing Co.: Tokyo, 1987; pp 77-206.

(38) Bruno, M.; Massaro, F. R.; Prencipe, M. *Surf. Sci.* **2008**, *602*, 2774-2782.

(39) Bruno, M.; Massaro, F. R.; Prencipe, M.; Aquilano, D. *CrystEngComm* **2010**, *12*, 3626-3633.

(40) Massaro, F. R.; Bruno, M.; Aquilano, D. *Cryst. Growth Des.* **2010**, *10*, 4096-4100.

(41) Massaro, F. R.; Rubbo, M.; Aquilano, D. *Cryst. Growth Des.* **2010**, *10*, 2870-2878.

(42) Haber, T.; Resel, R.; Thierry, A.; Campione, M.; Sassella, A.; Moret M. *Physica E* **2008**, *41*, 133-137.

(43) Campione, M.; Raimondo, L.; Moret, M.; Campiglio, P.; Fumagalli, E.; Sassella A. *Chem. Mater*. **2009,** *21*, 4859-4867.

(44) Raimondo, L.; Moret, M.; Campione, M.; Borghesi, A.; Sassella A. *J. Phys. Chem. C* **2011**, *115*, 5880-5885.

(45) Moret, M.; Borghesi, A.; Campione, M.; Fumagalli, E.; Raimondo, L.; Sassella A. *Cryst. Res. Technol.* **2011**, *46*, 827-832.

For Table of Contents Use Only

Equilibrium and growth morphology of oligoacenes: PBC analysis of naphthalene, anthracene and pentacene crystals

Francesco Roberto Massaro,[1] Massimo Moret,[1] Marco Bruno[2] and Dino Aquilano[2]*

[1] Dipartimento di Scienza dei Materiali – Università di Milano Bicocca,
via R.Cozzi 53, I-20125 Milano, Italy
[2] Dipartimento di Scienze Mineralogiche e Petrologiche – Università degli Studi di Torino,
via Valperga Caluso 35, I-10125 Torino, Italy

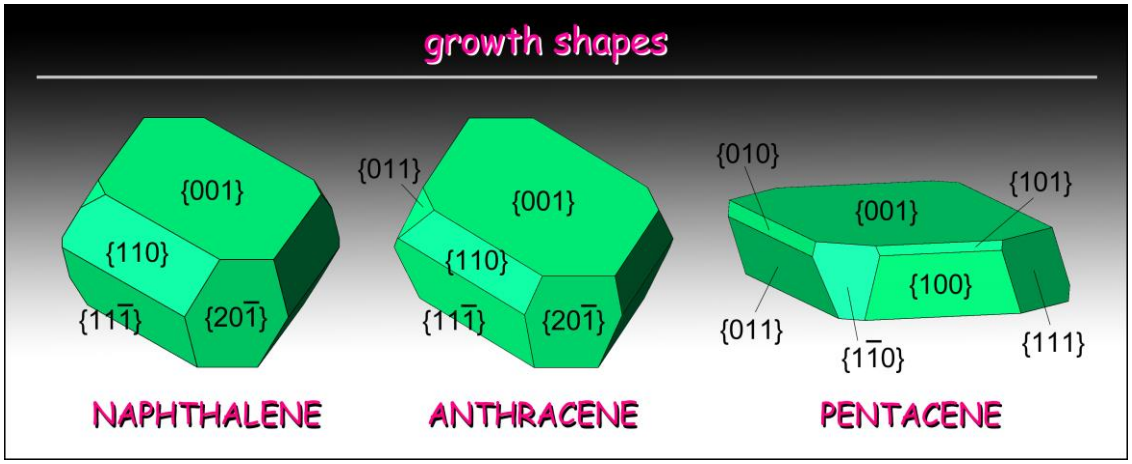

Synopsis

The athermal equilibrium and growth shapes of naphthalene, anthracene and pentacene crystals were calculated by using three different sets of empirical potentials (UNI, UFF and MM3 force fields). The surface profiles were obtained by applying the Hartman-Perdok method of the periodic bond chains. From calculations it ensues that surface relaxation only weakly affects surface and, even more, attachment energies of these semiconductor molecular crystals. It is noteworthy to point out that both equilibrium and growth shapes of these oligoacenes are quite similar when concerning phases belonging to the same point group.